



3 4456 0354621 4

ORNL/TM-11722

ornl

**OAK RIDGE
NATIONAL
LABORATORY**

MARTIN MARIETTA

Perturbed Environment Assessments for Space Vehicles

C. M. Haaland

OAK RIDGE NATIONAL LABORATORY

CENTRAL RESEARCH LIBRARY

CIRCULATION SECTION

4500N ROOM 115

LIBRARY LOAN COPY

DO NOT TRANSFER TO ANOTHER PERSON

If you wish someone else to see this
report, send in name with report and
the library will arrange a loan.

ORNL 7801 5 8 77

MANAGED BY
MARTIN MARIETTA ENERGY SYSTEMS, INC.
FOR THE UNITED STATES
DEPARTMENT OF ENERGY

This report has been reproduced directly from the best available copy.

Available to DOE and DOE contractors from the Office of Scientific and Technical Information, P.O. Box 62, Oak Ridge, TN 37831; prices available from (615) 576-8401. HTS 629-5027.

Available to the public from the Office of Technical Information, Service Center, Department of Commerce, 5205 Port Royal Pk., Springfield, VA 22151.

This report was prepared as an account of work sponsored by an agency of the United States Government. Neither the United States Government nor any agency thereof, nor any of their employees, makes any warranty, expressed or implied, or assumes any legal liability or responsibility for the accuracy, completeness, or usefulness of any information, product, or process disclosed, or represents that its use would not infringe privately owned rights. Reference herein to any specific commercial product, process, or service by trade name, trademark, manufacturer, or otherwise, does not necessarily constitute or imply its endorsement, recommendation, or favoring by the United States Government or any agency thereof. The views and opinions of authors expressed herein do not necessarily state or reflect those of the United States Government or any agency thereof.

ORNL/TM-11722

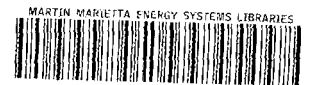
Engineering Physics and Mathematics

**PERTURBED ENVIRONMENT ASSESSMENTS FOR
SPACE VEHICLES**

Carsten M. Haaland

DATE PUBLISHED: June 1991

Prepared by the
OAK RIDGE NATIONAL LABORATORY
Oak Ridge, Tennessee 37831
managed by
MARTIN MARIETTA ENERGY SYSTEMS, INC.
for the
U.S. DEPARTMENT OF ENERGY
under contract DE-AC05-84OR21400



3 4456 0354621 4

TABLE OF CONTENTS

LIST OF FIGURES	v
LIST OF TABLES	vii
ABSTRACT	ix
EXECUTIVE SUMMARY	xii
1. INTRODUCTION	1
2. OVERVIEW OF PERTURBED EXOATMOSPHERIC ENVIRONMENT AND RESPONSE	3
3. EARLY-TIME BETA SPECTRUM FROM NUCLEAR DETONATIONS ..	7
3.1. Introduction	7
3.2. Comparison of Dickens' calculated data and previous data used	7
3.3. Comparison of experimental and calculated data	7
3.4. Which beta spectrum to use?	11
3.5. Conclusion and recommendation	11
4. HIGH-ENDOATMOSPHERIC X-RAY TRANSPORT MODELS	12
4.1. Introduction	12
4.2. XPORT programs	12
4.3. Comparison of results using ATR5 and XPRT5	15
4.3.1. Air density	15
4.3.2. Cross sections	17
4.3.3. Representation of BB spectra	17
4.4. Conclusion and recommendations	21
REFERENCES	24

LIST OF FIGURES

	<u>Page</u>
1. Comparison of normalized spectra for initial-time beta emission from fission of ^{235}U	8
2. Output from XPRT5 with additional parameters for comparison with ATR5. X-ray yield is one kiloton with a black-body temperature of 3.45 keV ($4 \times 10^7\text{K}$), altitude 150 kilofeet, range one kilometer, horizontal	14
3. Output from ATR5 for comparison with results from XPRT5 shown in Fig. 2 X-ray yield is one kiloton with a black-body temperature of 3.45 keV ($4 \times 10^7\text{K}$), altitude 150 kilofeet, range one kilometer, horizontal	20
4. Output from ATR5 for comparison with results from XPRT5 shown in Fig. 5. X-ray yield is one kiloton with a black-body temperature of 34.5 keV ($4 \times 10^8\text{K}$), altitude 100 kilofeet, range one kilometer, horizontal	22
5. Output from XPRT5 for comparison with results from ATR5 shown in Fig. 4. X-ray yield is one kiloton with a black-body temperature 34.5 keV ($4 \times 10^8\text{K}$), altitude 100 kilofeet, range one kilometer, horizontal	23

LIST OF TABLES

	<u>Page</u>
1. PERTURBED EXOATMOSPHERIC ENVIRONMENT AND RESPONSE. PART I & II	4
2. PERTURBED EXOATMOSPHERIC ENVIRONMENT AND RESPONSE. PART III	5
3. PERTURBED EXOATMOSPHERIC ENVIRONMENT AND RESPONSE PART IV & V	6
4. BETA SPECTRUM DATA AS PREVIOUSLY USED, FLATTENED AND NORMALIZED	9
5. DATA FROM DICKENS, 1982	10
6. COMPARISON BETWEEN ATR5 AND XPRT OF X-RAY TRANSPORT IN THE HIGH ENDOATMOSPHERE	16
7. COMPARISON BETWEEN ATR5 AND XPRT5 OF X-RAY CROSS SECTIONS IN	18
8. PHOTON ATTENUATION COEFFICIENTS COMPUTED FOR AIR	19

ABSTRACT

Three topics are discussed which are relevant to the technical assessment of the adequacy of environmental and response function analyses for space vehicles. First, a matrix is presented which summarizes exoatmospheric environmental modifiers and subsequent vehicular responses. Second, the early-time beta spectrum from a pulsed reactor experiment is compared with a beta spectrum which has been used for exoatmospheric analyses, showing that the average energy of the latter is significantly lower. Third, x-ray transport results are compared between ATR5 and XPRT5 for the high endoatmospheric regime (80 to 200 kilofeet altitude). Results are within less than 3% for altitudes of 150 kft and above, where the buildup factors are low, but differences up to 43% occur at lower altitudes. Possible reasons for these discrepancies are discussed.

EXECUTIVE SUMMARY

Three topics are discussed in this memorandum which are relevant to the technical assessment of the adequacy of environmental and response function analyses for space vehicles.

Topic 1: An overview of the problem is presented in the form of a matrix which summarizes all environmental modifiers and responses which may be of pertinence to the design of components for space vehicles. This matrix may be useful as a checklist for the comprehensiveness of space vehicle R&D programs. A subjective rating of the severity of response for each environmental modifier is listed. Response to the environmental effects of nuclear detonations in space are the most severe.

Topic 2: The early-time beta spectrum from fission which has been used for response analyses may be too low in energy. Recent data published on the beta spectrum from a pulsed reactor experiment are compared with data for the beta spectrum previously used for space vehicle analyses, showing that the average energy of the latter is significantly lower. A higher energy beta spectrum will produce a more severe response on critical optical sensors, and will affect the evaluation of beta energy pumpup by oscillations of the earth's magnetic field.

It is recommended that, before additional analyses are made involving this subject, a detailed research investigation should be made on the beta source spectrum and its variation with time during the first few minutes after a nuclear detonation. Future analyses on response of critical elements to betas should not be resumed until the beta spectrum controversy has been resolved.

Topic 3: The x-ray transport approximation, XPRT5, may be more suitable for high-endo analyses than ATR5. XPRT5 was designed specifically for high-endo application for the Air Force, whereas the ATR5 program was intended primarily for air-over-ground transport analyses of gamma-rays and neutrons. X-ray transport results are compared between ATR5 and XPRT5 for the high endoatmospheric regime (80 to 200 kilofeet altitude). Results agree within less than 3% for altitudes of 150 kft and above, where the buildup factors are low, but differences up to 43% occur at lower altitudes. Possible reasons for these discrepancies include a) more accurate air density estimates by XPRT5, b) more recent cross-section data used by XPRT5, and c) better representation of the black-body spectrum by XPRT5.

1. INTRODUCTION.

This memorandum discusses three topics related to the assessment of environmental modifiers and responses which may affect components of space vehicles. In Section 2, an overview of the space environment is presented in the form of a matrix which summarizes all environmental modifiers and responses which may result from perturbations to the exoatmosphere. This checklist may be useful for evaluating the comprehensiveness of R&D programs for space vehicles. In Section 3, the early-time beta spectrum from nuclear detonations is discussed. In Section 4, x-ray transport results are compared between ATR5 and XPRT5 for the high endoatmospheric regime (80 to 200 kilofeet altitude). Conclusions and recommendations are summarized in Section 5.

2. OVERVIEW OF PERTURBED EXOATMOSPHERIC ENVIRONMENT AND RESPONSE

In order to obtain an overview of the perturbed environment that is relevant to the design of components for space vehicles, a detailed matrix was developed which summarizes all space environmental modifiers and responses. In order to assure completeness, the list proceeds from nonmaterial modifiers consisting of static electric and magnetic fields and photons ranging in energy from low-frequency radio waves through cosmic rays, and then to material modifiers ranked from elementary particles up through entire objects.

The matrix is presented in three tables. Table 1 contains Part I which lists electric and magnetic fields, and Part II, which lists photons in order of increasing energy. Table 2 contains Part III which lists elementary, atomic and molecular particles, in order from smallest to largest mass. Table 3 contains Part IV, which lists debris, again from smallest to largest mass, and Part V, which lists various objects which may be encountered in space that maintain an identifiable integrity. Response and response severity have not been completed for Part V.

In addition to the potential environmental modifiers, the matrix lists the possible type of response, with a subjective evaluation of the severity of response graded on a scale from 1 to 10. The rating of "1" indicates that the response may not be serious, but it should be evaluated. The rating of "10" indicates total destruction to the object encountering the environmental modifier. The estimated severities entered into the matrix are not rigorous evaluations and are subject to reevaluation.

This matrix not only provides a complete listing of environmental considerations for the space defense vehicle, but also may be used as a systematic checklist to evaluate the thoroughness of survivability analyses of the space system.

Table 1. PERTURBED EXOATMOSPHERIC ENVIRONMENT AND RESPONSE. PARTS I & II.

LINE NO.	ENVIRONMENT CATEGORY	ENVIRONMENT SUBCATEGORY	SOURCE OF ENVIRONMENT	TYPE OF RESPONSE	RESPONSE SEVERITY
PART I. FIELDS					
1.	1. FIELDS	1.1. ELECTRIC	1.1.1. NUCLEAR DETONATION (NUDET)	1.1.1.1. ELECTRONIC	2
2.	1. FIELDS	1.1. ELECTRIC	1.1.2. SOLAR WIND	1.1.2.1. ELECTRONIC	1
3.	1. FIELDS	1.2. MAGNETIC	1.2.1. EARTH'S CORE	1.2.1.1. ELECTRONIC	1
4.	1. FIELDS	1.2. MAGNETIC	1.2.2. GEOPLASMA CURRENTS	1.2.2.1. ELECTRONIC	1
5.	1. FIELDS	1.2. MAGNETIC	1.2.3. NUDET DEBRIS MOTION	1.2.3.1. ELECTRONIC	1
PART II. PHOTONS					
1.	2. PHOTONS	2.1. RADIO ELF	2.1.1. MILITARY COMMUNICATIONS	2.1.1.1. ELECTRO INTERFERENCE	1
2.	2. PHOTONS	2.2. RADIO AM	2.2.1. COMMERCIAL BROADCAST	2.2.1.1. ELECTRO INTERFERENCE	1
3.	2. PHOTONS	2.3. RADIO FM	2.3.1. COMMERCIAL BROADCAST	2.3.1.1. ELECTRO INTERFERENCE	1
4.	2. PHOTONS	2.4. TV	2.4.1. COMMERCIAL BROADCAST	2.4.1.1. ELECTRO INTERFERENCE	1
5.	2. PHOTONS	2.5. SHORTWAVE	2.5.1. CIVIL COMMUNICATIONS	2.5.1.1. ELECTRONIC	1
6.	2. PHOTONS	2.5. SHORTWAVE	2.5.2. COMMERCIAL BROADCAST	2.5.2.1. ELECTRONIC	1
7.	2. PHOTONS	2.5. SHORTWAVE	2.5.3. MILITARY COMMUNICATIONS	2.5.3.1. ELECTRONIC	1
8.	2. PHOTONS	2.5. SHORTWAVE	2.5.4. HI-ALT EMP	2.5.4.1. CIRCUIT DAMAGE	8
9.	2. PHOTONS	2.6. MICROWAVE	2.6.1. COMMUNICATIONS	2.6.1.1. ELECTRO-INTERFERENCE	1
10.	2. PHOTONS	2.6. MICROWAVE	2.6.2. RADAR	2.6.2.1. ELECTRO-INTERFERENCE	1
11.	2. PHOTONS	2.7. SUBMILLIMETER	2.7.1. COMMUNICATIONS	2.7.1.1. ELECTRO-INTERFERENCE	1
12.	2. PHOTONS	2.7. SUBMILLIMETER	2.7.2. RADAR	2.7.2.1. DETECTION	1
13.	2. PHOTONS	2.8. INFRARED	2.8.1. COMMUNICATIONS (LASER)	2.8.1.1. INTERFERENCE	1
14.	2. PHOTONS	2.8. INFRARED	2.8.2. EARTH	2.8.2.1. INTERFERENCE	2
15.	2. PHOTONS	2.8. INFRARED	2.8.3. ILLUMINATION	2.8.3.1. DETECTION	1
16.	2. PHOTONS	2.8. INFRARED	2.8.4. MOON	2.8.4.1. INTERFERENCE	1
17.	2. PHOTONS	2.8. INFRARED	2.8.5. RADAR (LASER)	2.8.5.1. DETECTION	1
18.	2. PHOTONS	2.8. INFRARED	2.8.5. RADAR (LASER)	2.8.5.2. INTERFERENCE	2
19.	2. PHOTONS	2.8. INFRARED	2.8.6. NUDET THERMAL	2.8.6.1. SKIN HEATING	5
20.	2. PHOTONS	2.8. INFRARED	2.8.6. NUDET THERMAL	2.8.6.2. SKIN MELT	7
21.	2. PHOTONS	2.8. INFRARED	2.8.6. NUDET THERMAL	2.8.6.3. SHOCK & SPALLATION	10
22.	2. PHOTONS	2.8. INFRARED	2.8.7. SUN	2.8.7.1. INTERFERENCE	3
23.	2. PHOTONS	2.9. VISIBLE	2.9.1. COMMUNICATIONS (LASER)	2.9.1.1. INTERFERENCE	1
24.	2. PHOTONS	2.9. VISIBLE	2.9.2. EARTH	2.9.2.1. INTERFERENCE	2
25.	2. PHOTONS	2.9. VISIBLE	2.9.3. ILLUMINATION	2.9.3.1. DETECTION	1
26.	2. PHOTONS	2.9. VISIBLE	2.9.4. MOON	2.9.4.1. INTERFERENCE	1
27.	2. PHOTONS	2.9. VISIBLE	2.9.5. RADAR (LASER)	2.9.5.1. DETECTION	1
28.	2. PHOTONS	2.9. VISIBLE	2.9.5. RADAR (LASER)	2.9.5.2. INTERFERENCE	2
29.	2. PHOTONS	2.9. VISIBLE	2.9.6. NUDET THERMAL	2.9.6.1. SKIN HEATING	5
30.	2. PHOTONS	2.9. VISIBLE	2.9.6. NUDET THERMAL	2.9.6.2. SKIN MELT	7
31.	2. PHOTONS	2.9. VISIBLE	2.9.6. NUDET THERMAL	2.9.6.3. SHOCK & SPALLATION	10
32.	2. PHOTONS	2.9. VISIBLE	2.9.7. SUN	2.9.7.1. INTERFERENCE	3
33.	2. PHOTONS	2.10. ULTRAVIOLET	2.10.1. ILLUMINATION	2.10.1.1. DETECTION	1
34.	2. PHOTONS	2.10. ULTRAVIOLET	2.10.2. RADAR (LASER)	2.10.2.1. DETECTION	1
35.	2. PHOTONS	2.10. ULTRAVIOLET	2.10.2. RADAR (LASER)	2.10.2.2. INTERFERENCE	1
36.	2. PHOTONS	2.10. ULTRAVIOLET	2.10.3. NUDET THERMAL	2.10.3.1. SKIN HEATING	5
37.	2. PHOTONS	2.10. ULTRAVIOLET	2.10.3. NUDET THERMAL	2.10.3.2. SKIN MELT	7
38.	2. PHOTONS	2.10. ULTRAVIOLET	2.10.3. NUDET THERMAL	2.10.3.3. SHOCK & SPALLATION	10
39.	2. PHOTONS	2.10. ULTRAVIOLET	2.10.4. SUN	2.10.4.1. INTERFERENCE	3
40.	2. PHOTONS	2.11. X RAYS	2.11.1. NUDET THERMAL	2.11.1.1. LAYER HEATING	5
41.	2. PHOTONS	2.11. X RAYS	2.11.1. NUDET THERMAL	2.11.1.2. LAYER MELT	7
42.	2. PHOTONS	2.11. X RAYS	2.11.1. NUDET THERMAL	2.11.1.3. SECONDARY ELECTRONS	5
43.	2. PHOTONS	2.11. X RAYS	2.11.1. NUDET THERMAL	2.11.1.4. SPALLATION SHOCK	10
44.	2. PHOTONS	2.11. X RAYS	2.11.2. SUN	2.11.2.1. INTERFERENCE	3
45.	2. PHOTONS	2.12. GAMMA RAYS	2.12.1. NUDET FISS. DELAYED	2.12.1.1. ELECTRON PULSE	5
46.	2. PHOTONS	2.12. GAMMA RAYS	2.12.2. NUDET FISS. PROMPT	2.12.2.1. ELECTRON PULSE	5
47.	2. PHOTONS	2.12. GAMMA RAYS	2.12.3. NUDET NEUTRON CAPTURE	2.12.3.1. ELECTRON PULSE	5
48.	2. PHOTONS	2.12. GAMMA RAYS	2.12.4. SUN	2.12.4.1. CIRCUIT NOISE	3
49.	2. PHOTONS	2.13. COSMIC RAYS	2.13.1. SOLAR & GALACTIC	2.13.1.1. CIRCUIT NOISE	1

Table 2. PERTURBED EXOATMOSPHERIC ENVIRONMENT AND RESPONSE. PART III.

LINE NO.	ENVIRONMENT CATEGORY	ENVIRONMENT SUBCATEGORY	SOURCE OF ENVIRONMENT	TYPE OF RESPONSE	RESPONSE SEVERITY
1.	3. PARTICLES	3.1. ELECTRONS	3.1.1. IONOSPHERE	3.1.1.1. CIRCUIT NOISE	1
2.	3. PARTICLES	3.1. ELECTRONS	3.1.1. IONOSPHERE	3.1.1.2. SENS.COMP.DAMAGE	2
3.	3. PARTICLES	3.1. ELECTRONS	3.1.2. NUDET BETAS	3.1.2.1. CIRCUIT NOISE	5
4.	3. PARTICLES	3.1. ELECTRONS	3.1.2. NUDET BETAS	3.1.2.2. SENS.COMP.DAMAGE	7
5.	3. PARTICLES	3.1. ELECTRONS	3.1.3. SECONDARIES	3.1.3.1. CIRCUIT NOISE	2
6.	3. PARTICLES	3.1. ELECTRONS	3.1.3. SECONDARIES	3.1.3.2. SENS.COMP.DAMAGE	3
7.	3. PARTICLES	3.1. ELECTRONS	3.1.4. SOLAR WIND	3.1.4.1. CIRCUIT NOISE	1
8.	3. PARTICLES	3.1. ELECTRONS	3.1.4. SOLAR WIND	3.1.4.2. SENS.COMP.DAMAGE	2
9.	3. PARTICLES	3.1. ELECTRONS	3.1.5. TRAPPED, MAGNETOSPHERE	3.1.5.1. CIRCUIT NOISE	4
10.	3. PARTICLES	3.1. ELECTRONS	3.1.5. TRAPPED, MAGNETOSPHERE	3.1.5.2. SENS.COMP.DAMAGE	5
11.	3. PARTICLES	3.2. POSITRONS	3.2.1. PAIR PRODUCTION	3.2.1.1. CIRCUIT NOISE	1
12.	3. PARTICLES	3.3. PROTONS	3.3.1. IONOSPHERE	3.3.1.1. CIRCUIT NOISE	1
13.	3. PARTICLES	3.3. PROTONS	3.3.1. IONOSPHERE	3.3.1.2. SENS.COMP.DAMAGE	2
14.	3. PARTICLES	3.3. PROTONS	3.3.2. NUDET	3.3.2.1. CIRCUIT NOISE	5
15.	3. PARTICLES	3.3. PROTONS	3.3.2. NUDET	3.3.2.2. SENS.COMP.DAMAGE	6
16.	3. PARTICLES	3.3. PROTONS	3.3.3. SOLAR WIND	3.3.3.1. CIRCUIT NOISE	1
17.	3. PARTICLES	3.3. PROTONS	3.3.3. SOLAR WIND	3.3.3.2. SENS.COMP.DAMAGE	2
18.	3. PARTICLES	3.3. PROTONS	3.3.4. TRAPPED, MAGNETOSPHERE	3.3.4.1. CIRCUIT NOISE	3
19.	3. PARTICLES	3.3. PROTONS	3.3.4. TRAPPED, MAGNETOSPHERE	3.3.4.2. SENS.COMP.DAMAGE	4
20.	3. PARTICLES	3.4. NEUTRONS	3.4.2. NUDET	3.4.2.1. CIRCUIT NOISE	5
21.	3. PARTICLES	3.4. NEUTRONS	3.4.2. NUDET	3.4.2.2. SENS.COMP.DAMAGE	6
22.	3. PARTICLES	3.4. NEUTRONS	3.4.2. NUDET	3.4.2.3. PIT MELT	9
23.	3. PARTICLES	3.4. NEUTRONS	3.4.2. NUDET	3.4.2.4. PIT SHOCK & SPALL	10
24.	3. PARTICLES	3.4. NEUTRONS	3.4.3. SOLAR WIND	3.4.3.1. CIRCUIT NOISE	1
25.	3. PARTICLES	3.4. NEUTRONS	3.4.3. SOLAR WIND	3.4.3.2. SENS.COMP.DAMAGE	2
26.	3. PARTICLES	3.5. MUONS	3.5.1. COSMIC RADIATION	3.5.1.1. CIRCUIT NOISE	1
27.	3. PARTICLES	3.6. IONS, NEGATIVE	3.6.1. COMET OR METEOR	3.6.1.1. CIRCUIT NOISE	1
28.	3. PARTICLES	3.6. IONS, NEGATIVE	3.6.1. COMET OR METEOR	3.6.1.2. SENS.COMP.DAMAGE	2
29.	3. PARTICLES	3.6. IONS, NEGATIVE	3.6.2. IONOSPHERE	3.6.2.1. CIRCUIT NOISE	1
30.	3. PARTICLES	3.6. IONS, NEGATIVE	3.6.3. NUDET	3.6.3.1. CIRCUIT NOISE	5
31.	3. PARTICLES	3.6. IONS, NEGATIVE	3.6.3. NUDET	3.6.3.2. SENS.COMP.DAMAGE	6
32.	3. PARTICLES	3.6. IONS, NEGATIVE	3.6.4. SOLAR WIND	3.6.4.1. CIRCUIT NOISE	1
33.	3. PARTICLES	3.7. IONS, POSITIVE	3.7.1. COMET OR METEOR	3.7.1.1. CIRCUIT NOISE	1
34.	3. PARTICLES	3.7. IONS, POSITIVE	3.7.1. COMET OR METEOR	3.7.1.2. SENS.COMP.DAMAGE	2
35.	3. PARTICLES	3.7. IONS, POSITIVE	3.7.2. IONOSPHERE	3.7.2.1. CIRCUIT NOISE	1
36.	3. PARTICLES	3.7. IONS, POSITIVE	3.7.3. NUDET	3.7.3.1. CIRCUIT NOISE	5
37.	3. PARTICLES	3.7. IONS, POSITIVE	3.7.3. NUDET	3.7.3.2. SENS.COMP.DAMAGE	6
38.	3. PARTICLES	3.7. IONS, POSITIVE	3.7.4. SOLAR WIND	3.7.4.1. CIRCUIT NOISE	1
39.	3. PARTICLES	3.8. ATOMS	3.8.1. ATMOSPHERE	3.8.1.1. CIRCUIT NOISE	1
40.	3. PARTICLES	3.8. ATOMS	3.8.2. COMET OR METEOR	3.8.2.1. CIRCUIT NOISE	1
41.	3. PARTICLES	3.8. ATOMS	3.8.2. COMET OR METEOR	3.8.2.2. SENS.COMP.DAMAGE	2
42.	3. PARTICLES	3.8. ATOMS	3.8.3. NUDET	3.8.3.1. CIRCUIT NOISE	5
43.	3. PARTICLES	3.8. ATOMS	3.8.3. NUDET	3.8.3.2. SENS.COMP.DAMAGE	6
44.	3. PARTICLES	3.8. ATOMS	3.8.4. SOLAR WIND	3.8.4.1. CIRCUIT NOISE	1
45.	3. PARTICLES	3.9. MOLECULES	3.9.1. ATMOSPHERE	3.9.1.1. CIRCUIT NOISE	1
46.	3. PARTICLES	3.9. MOLECULES	3.9.2. COMET OR METEOR	3.9.2.1. CIRCUIT NOISE	1
47.	3. PARTICLES	3.9. MOLECULES	3.9.2. COMET OR METEOR	3.9.2.2. SENS.COMP.DAMAGE	2
48.	3. PARTICLES	3.9. MOLECULES	3.9.3. NUDET	3.9.3.1. CIRCUIT NOISE	5
49.	3. PARTICLES	3.9. MOLECULES	3.9.3. NUDET	3.9.3.2. SENS.COMP.DAMAGE	6
50.	3. PARTICLES	3.9. MOLECULES	3.9.4. SOLAR WIND	3.9.4.1. CIRCUIT NOISE	1

Table 3. PERTURBED EXOATMOSPHERIC ENVIRONMENT AND REPOSE. PARTS IV & V.

LINE NO.	ENVIRONMENT CATEGORY	ENVIRONMENT SUBCATEGORY	SOURCE OF ENVIRONMENT	TYPE OF RESPONSE	RESPONSE SEVERITY
PART IV. DEBRIS					
1.	4. DEBRIS	4.1. SUB-MICRON	4.1.1. COMET OR METEOR	4.1.1.1. EROSION	1
2.	4. DEBRIS	4.1. SUB-MICRON	4.1.3. HIGH EXPL. INTERCEPT	4.1.3.1. EROSION	5
3.	4. DEBRIS	4.1. SUB-MICRON	4.1.4. KINETIC ENERGY INTERCEPT	4.1.4.1. EROSION	5
4.	4. DEBRIS	4.1. SUB-MICRON	4.1.5. NUDET	4.1.5.1. EROSION	5
5.	4. DEBRIS	4.1. SUB-MICRON	4.1.5. NUDET	4.1.5.2. SURFACE MELT	6
6.	4. DEBRIS	4.1. SUB-MICRON	4.1.6. RE-ENTRY BREAKUP	4.1.6.1. EROSION	5
7.	4. DEBRIS	4.2. MICRON	4.2.1. COMET OR METEOR	4.2.1.1. EROSION	1
8.	4. DEBRIS	4.2. MICRON	4.2.1. COMET OR METEOR	4.2.1.2. SURFACE HOLES	2
9.	4. DEBRIS	4.2. MICRON	4.2.3. HE INTERCEPT	4.2.3.1. EROSION	5
10.	4. DEBRIS	4.2. MICRON	4.2.3. HE INTERCEPT	4.2.3.2. SURFACE HOLES	6
11.	4. DEBRIS	4.2. MICRON	4.2.4. KINETIC ENERGY INTERCEPT	4.2.4.1. EROSION	5
12.	4. DEBRIS	4.2. MICRON	4.2.4. KINETIC ENERGY INTERCEPT	4.2.4.2. SURFACE HOLES	6
13.	4. DEBRIS	4.2. MICRON	4.2.5. NUDET	4.2.5.1. EROSION	5
14.	4. DEBRIS	4.2. MICRON	4.2.5. NUDET	4.2.5.2. SURFACE HOLES	6
15.	4. DEBRIS	4.2. MICRON	4.2.5. NUDET	4.2.5.3. SURFACE MELT	7
16.	4. DEBRIS	4.2. MICRON	4.2.6. RE-ENTRY BREAKUP	4.2.6.1. EROSION	6
17.	4. DEBRIS	4.2. MICRON	4.2.6. RE-ENTRY BREAKUP	4.2.6.2. SURFACE HOLES	7
18.	4. DEBRIS	4.3. SUBMILLIMETER	4.3.1. COMET OR METEOR	4.3.1.1. EROSION	6
19.	4. DEBRIS	4.3. SUBMILLIMETER	4.3.1. COMET OR METEOR	4.3.1.2. SURFACE HOLES	7
20.	4. DEBRIS	4.3. SUBMILLIMETER	4.3.1. COMET OR METEOR	4.3.1.3. COMPONENT DAMAGE	2
21.	4. DEBRIS	4.3. SUBMILLIMETER	4.3.3. HE INTERCEPT	4.3.1.1. EROSION	5
22.	4. DEBRIS	4.3. SUBMILLIMETER	4.3.3. HE INTERCEPT	4.3.1.2. SURFACE HOLES	6
23.	4. DEBRIS	4.3. SUBMILLIMETER	4.3.3. HE INTERCEPT	4.3.1.3. COMPONENT DAMAGE	5
24.	4. DEBRIS	4.3. SUBMILLIMETER	4.3.4. KINETIC ENERGY INTERCEPT	4.3.1.1. EROSION	5
25.	4. DEBRIS	4.3. SUBMILLIMETER	4.3.4. KINETIC ENERGY INTERCEPT	4.3.1.2. SURFACE HOLES	6
26.	4. DEBRIS	4.3. SUBMILLIMETER	4.3.4. KINETIC ENERGY INTERCEPT	4.3.1.3. COMPONENT DAMAGE	5
27.	4. DEBRIS	4.3. SUBMILLIMETER	4.3.5. NUDET	4.3.1.1. EROSION	5
28.	4. DEBRIS	4.3. SUBMILLIMETER	4.3.5. NUDET	4.3.1.2. SURFACE HOLES	6
29.	4. DEBRIS	4.3. SUBMILLIMETER	4.3.5. NUDET	4.3.1.3. COMPONENT DAMAGE	7
30.	4. DEBRIS	4.3. SUBMILLIMETER	4.3.5. NUDET	4.3.5.4. SHOCK & SPALLATION	8
31.	4. DEBRIS	4.3. SUBMILLIMETER	4.3.6. RE-ENTRY BREAKUP	4.3.1.1. EROSION	5
32.	4. DEBRIS	4.3. SUBMILLIMETER	4.3.6. RE-ENTRY BREAKUP	4.3.1.2. SURFACE HOLES	6
33.	4. DEBRIS	4.3. SUBMILLIMETER	4.3.6. RE-ENTRY BREAKUP	4.3.1.3. COMPONENT DAMAGE	7
34.	4. DEBRIS	4.4. FRAGMENTS	4.4.1. COMET OR METEOR	4.4.1.1. SURFACE HOLES	5
35.	4. DEBRIS	4.4. FRAGMENTS	4.4.1. COMET OR METEOR	4.4.1.2. DESTRUCTION	10
36.	4. DEBRIS	4.4. FRAGMENTS	4.4.2. HE INTERCEPT	4.4.3.1. SURFACE HOLES	5
37.	4. DEBRIS	4.4. FRAGMENTS	4.4.2. HE INTERCEPT	4.4.3.2. DESTRUCTION	10
38.	4. DEBRIS	4.4. FRAGMENTS	4.4.3. KINETIC ENERGY INTERCEPT	4.4.1.1. SURFACE HOLES	5
39.	4. DEBRIS	4.4. FRAGMENTS	4.4.3. KINETIC ENERGY INTERCEPT	4.4.1.2. DESTRUCTION	10
40.	4. DEBRIS	4.4. FRAGMENTS	4.4.4. NUDET	4.4.3.1. SURFACE HOLES	5
41.	4. DEBRIS	4.4. FRAGMENTS	4.4.4. NUDET	4.4.3.2. DESTRUCTION	10
42.	4. DEBRIS	4.4. FRAGMENTS	4.4.5. RE-ENTRY BREAKUP	4.4.3.1. SURFACE HOLES	5
43.	4. DEBRIS	4.4. FRAGMENTS	4.4.5. RE-ENTRY BREAKUP	4.4.3.2. DESTRUCTION	10
PART V. OBJECTS					
1.	5. OBJECTS	5.1. CHAFF			
2.	5. OBJECTS	5.2. COMET OR METEOR			
3.	5. OBJECTS	5.3. DECOYS			
4.	5. OBJECTS	5.4. MISSILES			
5.	5. OBJECTS	5.5. BOOSTERS, ETC.			
6.	5. OBJECTS	5.6. SATELLITES			

3. EARLY-TIME BETA SPECTRUM FROM NUCLEAR DETONATIONS

3.1. Introduction. The early-time (first few seconds) beta spectrum is of interest for analyses of the possible buildup in energy of trapped betas due to expansion and squeezing oscillations of the earth's geomagnetic sphere resulting from nuclear detonations in the exoatmosphere. Data used for previous analyses¹ of this subject were analyzed and compared in detail with data from a paper by Dickens.² A plot of the normalized data, as shown in Fig. 1, shows the betas in the 3 to 6 MeV range being 1.5 to 5 times greater in quantity in the Dickens' data than in the data previously used for space analyses. These additional high energy betas may have impact on analyses for the design of critical components.

3.2. Comparison of Dickens' calculated data and previous data used: The previously used data for space analyses show a decrease in flux at beta energies below about 0.8 MeV, and presumably ends at 0.2 MeV, as listed in Table 4. This behavior corresponds with the curve using calculations based on ENDF/B-V shown as a solid line in Figure 2 of reference 2. The actual data used by Dickens are no longer available, hence the calculations presented here are based on visual estimates taken from an enlarged version of Figure 2 of reference 2. These data points are listed in Table 5. The calculated average beta energy is 1.96 MeV. This energy is for a time of 1.7 s after the uranium is exposed to neutrons, corresponding to 1.7 s after detonation of a uranium fission weapon.

If the time-dependency relationship for E_{av} given on p. 71 of the TREM TECHNICAL MANUAL, Volume II (reference 3) is used to extrapolate this 1.96 MeV back to zero time, then the INITIAL average beta energy comes to 2.14 MeV, 36% higher than the 1.57 MeV obtained from the previously used beta data.¹

3.3. Comparison of experimental and calculated data: Figure 2 of Dickens' paper shows that experimental measurement of the beta flux (after a wait of 1.7 seconds after exposure of ²³⁵U to a pulse of neutrons) for energies below 1 MeV produces a nearly FLAT curve down to about 0.2 MeV, whereas the solid curve based on theoretical evaluation from ENDF/B-V data shows a falloff in flux below about 0.8 MeV, as do the previously used beta data also. The fault is attributed to incomplete ENDF data, which results partly due to experimental difficulties in this realm of the spectrum. Efforts are underway at various laboratories on the preparation of ENDF/B-VI, which may remove some of this discrepancy. The experimental data in Dickens' Figure 2 ends at 0.2 MeV primarily because of experimental difficulties in

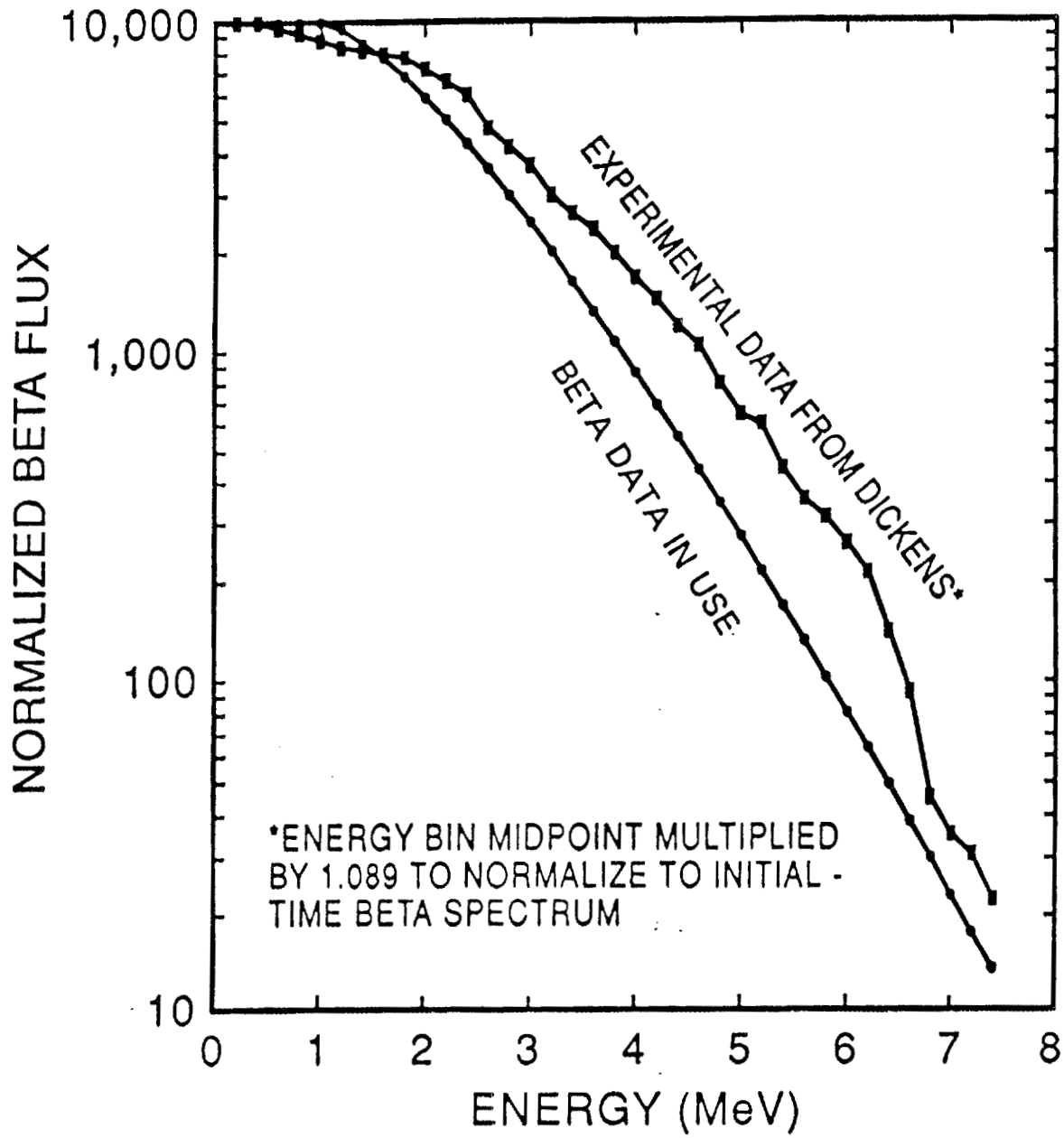


Figure 1. Comparison of normalized spectra for initial-time beta emission from fission of ^{235}U .

TABLE 4. Beta spectrum data as previously used, flattened and normalized

Energy bin midpoint (MeV)	Beta data as used	Flattened spectrum	Flattened spectrum normalized to 10,000
0.25	572.00	860.00	
0.4	677.00	860.00	9999.99
0.6	808.00	860.00	9999.99
0.8	859.00	859.00	9988.37
1.0	855.00	855.00	9941.85
1.2	813.00	813.00	9453.48
1.4	748.00	748.00	8697.67
1.6	672.00	672.00	7813.95
1.8	591.00	591.00	6872.09
2.0	512.00	512.00	5953.48
2.2	438.00	438.00	5093.02
2.4	370.00	370.00	4302.32
2.6	310.00	310.00	3604.65
2.8	257.00	257.00	2988.37
3.0	212.00	212.00	2465.11
3.2	174.00	174.00	2023.25
3.4	141.00	141.00	1639.53
3.6	114.00	114.00	1325.58
3.8	92.20	92.20	1072.09
4.0	74.00	74.00	860.46
4.2	59.10	59.10	687.21
4.4	47.10	47.10	547.67
4.6	37.40	37.40	434.88
4.8	29.60	29.60	344.19
5.0	23.40	23.40	272.09
5.2	18.40	18.40	213.95
5.4	14.40	14.40	167.44
5.6	11.30	11.30	131.40
5.8	8.84	8.84	102.79
6.0	6.90	6.90	80.23
6.2	5.37	5.37	62.44
6.4	4.18	4.18	48.60
6.6	3.24	3.24	37.67
6.8	2.51	2.51	29.19
7.0	1.94	1.94	22.56
7.2	1.50	1.50	17.44
7.4	1.16	1.16	13.49

Average energy for beta data as used, 1.578205 MeV
 Average energy with flattened spectrum to zero energy, 1.448404 MeV

Table 5. Data from Dickens, 1982 (see text).

Energy bin midpoint (MeV)	Experimental data estimated from graph	Calculated data estimated from graph	Experimental data normalized to 10,000
0.2	2500.0	1350.0	10000.0
0.4	2500.0	1550.0	10000.0
0.6	2400.0	1800.0	9600.0
0.8	2300.0	2000.0	9200.0
1.0	2200.0	2100.0	8800.0
1.2	2100.0	2100.0	8400.0
1.4	2050.0	2050.0	8200.0
1.6	2000.0	2000.0	8000.0
1.8	1950.0	1950.0	7800.0
2.0	1800.0	1800.0	7200.0
2.2	1650.0	1650.0	6600.0
2.4	1500.0	1500.0	6000.0
2.6	1200.0	1250.0	4800.0
2.8	1050.0	1150.0	4200.0
3.0	920.0	1000.0	3680.0
3.2	750.0	900.0	3000.0
3.4	660.0	780.0	2640.0
3.6	590.0	660.0	2360.0
3.8	500.0	550.0	2000.0
4.0	420.0	460.0	1680.0
4.2	360.0	400.0	1440.0
4.4	300.0	320.0	1200.0
4.6	260.0	275.0	1040.0
4.8	200.0	220.0	800.0
5.0	160.0	180.0	640.0
5.2	150.0	150.0	600.0
5.4	110.0	115.0	440.0
5.6	88.0	90.0	352.0
5.8	78.0	75.0	312.0
6.0	65.0	58.0	260.0
6.2	53.0	45.0	212.0
6.4	35.0	35.0	140.0
6.6	23.0	28.0	92.0
6.8	11.0	21.0	44.0
7.0	8.6	15.0	34.4
7.2	7.5	11.0	30.0
7.4	5.5	8.0	22.0
7.6	2.0	5.0	8.0
7.8	0.0	2.6	0.0
8.0	0.0	1.0	0.0

AVERAGE ENERGY FOR EXPERIMENTAL DATA, 1.775805 MeV
 AVERAGE ENERGY FOR CALCULATED DATA, 1.958769 MeV
 AVERAGE ENERGY FOR FLATTENED SPECTRUM TO ZERO ENERGY, 1.712395 MeV

making measurements at lower energy. These lower energy betas are of less significance than the higher energy betas for analyzing response of sensitive space vehicle components, and can probably be neglected for that application. However, the presence of these lower energy betas can significantly affect the calculated result obtained for the mean energy of the beta spectrum.

3.4. Which beta spectrum to use? Because of the effect of low energy betas on the estimated mean energy, and as a conclusion resulting from the discussion given above, it should probably be assumed that the beta spectrum is FLAT from about 0.8 MeV down to almost zero energy. With this assumption, the previously used beta data average to 1.45 MeV. The Dickens paper experimental data average to 1.71 MeV, which becomes 1.86 MeV when adjusted to initial time (multiplying energy by $(1+t)^{0.086}$, according to the TREM manual³, with $t=1.7$ seconds). The difference between an average energy of 1.45 and 1.86 MeV may seem inconsequential, but when the two spectra are plotted, as shown in Figure 1, the difference in the SHAPES of the spectra are significant. The normalization of the two curves is an approximation because the curves were not integrated to obtain the same total number of betas for each curve. On visual inspection of the two curves, it is apparent that a detailed normalization would shift the experimental data from Dickens upwards slightly to make the two curves even more separated.

3.5. Conclusions and recommendation: Incorporation of the revised beta spectrum as presented here may have a significant effect on radiation analyses concerning durability of optical components for space vehicles. *It is recommended that a detailed research investigation should be made on the beta source spectrum, as well as its variation with time, before additional analyses are made on this subject.*

4. HIGH-ENDOATMOSPHERIC X-RAY TRANSPORT MODELS

4.1. Introduction. One of the computational programs in the inventory for calculating radiation transport is the ATR5 code.⁴ This code is intended for analyses of transport in air of gamma rays, neutrons, and x rays from nuclear detonations. The RSIC document⁴ states on page iv, "Accuracy is poor for source-target combinations above 20 km." For high endoatmospheric x-ray transport analyses, the XPORT series of programs developed at ORNL may be more accurate and appropriate than ATR5. Comparison of results and a discussion of model strengths and deficiencies are presented here.

The XPORT series of programs are quick-running computational codes generated for the Air Force Wright Aeronautical Laboratories to provide overviews to the problem of potential x-ray damage to Air Force vehicles. Altitudes of interest for this problem range from 80 - 200 kilofeet (24.4 - 61 km). A series of programs were constructed around a simplified method developed for approximating the air-transported x-ray spectrum from nuclear detonations in the atmosphere. Details of the theory, methodology, calibration and results are described in *Applied Radiation and Isotopes*.⁵

The XPORT code is briefly described in section 5.2. Results of computations obtained by XPRT5, a specific version of XPORT, and ATR5, for two black-body temperatures, four altitudes, and three horizontal ranges from source to target, are presented in section 5.3.

4.2. XPORT programs. The XPORT simplification reduces computational time such that a desk-top computer can provide results that match detailed Monte Carlo calculations within $\pm 10\%$ for a wide range of conditions. The approximation requires a fraction of a second with a modern desk-top computer whereas the comparable calculation using the Monte Carlo code typically requires 10 - 15 seconds on a Cray computer. This simplification makes feasible iterative calculations to obtain constrained solutions which would be prohibitively costly otherwise.

The method consists of (1) representing the black-body continuous spectrum by 25 discrete emission windows, (2) consulting tables of photon buildup factors in air for the discrete emission energies, (3) unfolding the buildup photons by using air kerma response functions and an assumption for redistributing the photons to windows of lower energy, and (4) applying cutoff and weighing factors to improve the correlation with Monte Carlo benchmark calculations.

The emission windows are calculated for each selected black-body temperature so that 16 windows cover the energies above the peak emission frequency and 8 windows cover energies at lower frequencies. This process assures an optimum coverage of the Planck spectrum by energy bins for any black-body temperature.

Attenuation coefficients for photons were computed for air using the PHOTX library of the National Institute of Standards and Technology, which will be used as the basis of File 23 for ENDF/B-VI.⁶ Only the first four most abundant constituents of the sea-level atmosphere (US Standard, 1976) were used to construct the table of photon attenuation coefficients, using volumes of 78.085% for N₂, 20.948% for O₂, 0.935% for Ar, and 0.032% for CO₂. The attenuation coefficient for a given photon energy is calculated by log-log extrapolation from a table, which includes 38 photon energies from 1 keV through 10 MeV. Detailed k-shell photo-absorption data from the PHOTX library were not included.

To provide accuracy in calculating the x-ray mean free path lengths in the upper atmosphere, the integrated air path density is calculated by exponential interpolation between 90 data points from the U.S. Standard Atmosphere, 1976, for altitudes between ground and 300 km.

Monte Carlo benchmarks were calculated for 24 cases, namely black-body temperatures of 4×10^7 and 4×10^8 K (3.45 and 34.5 keV), atmospheric densities corresponding to 80, 100, 150 and 200 kft (24.384, 30.48, 45.72, and 60.96 km, respectively) altitudes, and ranges of 1, 2 and 4 km. Comparisons of the integrated energies and photon fluxes for the 24 cases are shown in reference 5. The percent deviation of the results of the approximation from those of the MCNP Monte Carlo calculation are less than 10% for 20 out of 24 cases for the energy, and for 19 out of 24 cases for the flux. The approximation does not provide good results when over half of the emission channels become nontransmitting due to a large number of mean free paths (>12). The approximation code provides a warning when this situation occurs. For applications for the USAF, involving interception analyses in the high endoatmosphere by x rays from nuclear detonations, this warning was rarely encountered.

Detailed spectral comparisons between the results of the XPORT approximation and the Monte Carlo runs are illustrated in reference 5.

A sample output of one of the x-ray transport programs (XPRT5) is illustrated in Fig. 2. The input parameters are entered during a question and answer session between the machine and the user. Input includes yield, black-body temperature, fraction of yield in x rays, range from weapon to target, altitude of target, and slant angle to horizontal of the range vector from the warhead.

INPUT: Yield of nuclear warhead: 1 kilotons; Fraction of yield emitted as x rays: 1
 Blackbody x-ray temperature: 3.44693 keV (4E+07 deg. Kelvin)
 Altitude of target: 150 kilofeet (45.72 kilometers)
 Slant range to detonation: 1 kilometers
 Slant angle (to horizontal) from target to detonation: 0 degrees
 OUTPUT: Height of detonation above or below (negative) target: 0 kilofeet
 Air density at target altitude: 1.781716E-06 gm/cm³
 Integrated air mass along slant path: .1781716 gm/cm²
 Total unattenuated x ray deposition at target: 7.957747 cal/cm²
 Photon energy at peak emission power: 9.725301 keV
 Total x-ray energy output: 2.609E+28 keV; Total number of source x-ray photons, 2.678387E+27
 Number of transmitting windows: 23
 PARAM = 1.953952 ; G = 3.614444

ENERGY DEPOSITION PER WINDOW:

Percent of source energy	Photon energy (keV)	Mu (cm ² /gm)	Number of HFPs	Buildup factor	Uncollided flux (Energy) (cal/cm ²)	Fraction of total uncoll. flux (Photons) (#/cm ²)	Flux w/buildup (Energy) (cal/cm ²)	Fraction of total (Photons) (#/cm ²)	Photon buildup	No. of source photons	Photons per vacuum photon		
0.2250	46.25	2.21E-01	3.95E-02	1.0705E+00	0.02	9.709E+12	0.004	0.018	1.022E+13	0.004	1.0522	1.269E+24	1.012E+00
0.3125	38.70	2.59E-01	4.62E-02	1.0727E+00	0.02	1.601E+13	0.006	0.025	1.672E+13	0.006	1.0448	2.107E+24	9.977E-01
0.3125	35.96	2.84E-01	5.05E-02	1.0731E+00	0.02	1.716E+13	0.006	0.025	1.784E+13	0.006	1.0398	2.267E+24	9.887E-01
0.6250	33.49	3.09E-01	5.51E-02	1.0735E+00	0.05	3.667E+13	0.012	0.049	3.836E+13	0.012	1.0460	4.869E+24	9.900E-01
0.6250	31.47	3.34E-01	5.95E-02	1.0738E+00	0.05	3.885E+13	0.012	0.049	4.051E+13	0.011	1.0427	5.181E+24	9.826E-01
1.2500	29.40	3.68E-01	6.56E-02	1.0742E+00	0.09	8.267E+13	0.023	0.098	8.674E+13	0.023	1.0492	1.109E+25	9.827E-01
1.2500	27.50	4.19E-01	7.47E-02	1.0749E+00	0.09	8.759E+13	0.023	0.097	9.162E+13	0.023	1.0460	1.186E+25	9.708E-01
2.5000	25.49	4.86E-01	8.65E-02	1.0751E+00	0.18	1.867E+14	0.045	0.192	1.967E+14	0.045	1.0534	2.558E+25	9.662E-01
2.5000	23.59	5.65E-01	1.01E-01	1.0743E+00	0.18	1.990E+14	0.044	0.189	2.089E+14	0.044	1.0499	2.765E+25	9.495E-01
5.0000	21.52	6.75E-01	1.20E-01	1.0719E+00	0.35	4.278E+14	0.087	0.373	4.521E+14	0.088	1.0567	6.063E+25	9.370E-01
5.0000	19.49	8.31E-01	1.48E-01	1.0692E+00	0.34	4.594E+14	0.085	0.361	4.833E+14	0.085	1.0521	6.693E+25	9.074E-01
5.0000	17.91	1.03E+00	1.83E-01	1.0707E+00	0.33	4.827E+14	0.082	0.349	5.080E+14	0.082	1.0525	7.285E+25	8.782E-01
5.0000	16.59	1.25E+00	2.23E-01	1.0705E+00	0.32	5.011E+14	0.079	0.336	5.280E+14	0.079	1.0538	7.865E+25	8.436E-01
10.0000	14.91	1.64E+00	2.92E-01	1.0671E+00	0.59	1.040E+15	0.147	0.631	1.105E+15	0.148	1.0619	1.750E+26	7.930E-01
10.0000	13.00	2.42E+00	4.31E-01	1.0605E+00	0.52	1.037E+15	0.128	0.546	1.095E+15	0.128	1.0556	2.006E+26	6.860E-01
10.0000	11.32	3.60E+00	6.41E-01	1.0350E+00	0.42	9.665E+14	0.103	0.436	1.006E+15	0.103	1.0410	2.306E+26	5.484E-01
10.0000	9.73	5.56E+00	9.91E-01	1.0085E+00	0.30	7.927E+14	0.073	0.301	8.072E+14	0.071	1.0182	2.683E+26	3.781E-01
10.0000	8.13	9.45E+00	1.68E+00	1.0020E+00	0.15	4.740E+14	0.036	0.149	4.770E+14	0.035	1.0063	3.208E+26	1.868E-01
5.0000	6.86	1.57E+01	2.80E+00	1.0000E+00	0.02	9.195E+13	0.006	0.024	9.215E+13	0.006	1.0022	1.903E+26	6.085E-02
5.0000	5.91	2.45E+01	4.37E+00	1.0000E+00	0.01	2.228E+13	0.001	0.005	2.231E+13	0.001	1.0012	2.208E+26	1.269E-02
2.5000	5.09	3.81E+01	6.79E+00	1.0000E+00	0.00	1.143E+12	0.000	0.000	1.144E+12	0.000	1.0011	1.280E+26	1.123E-03
2.5000	4.46	5.64E+01	1.00E+01	1.0000E+00	0.00	5.069E+10	0.000	0.000	5.078E+10	0.000	1.0017	1.461E+26	4.367E-05
2.5000	3.70	9.51E+01	1.69E+01	1.0000E+00	0.00	6.143E+07	0.000	0.000	6.207E+07	0.000	1.0104	1.764E+26	4.423E-08
2.5000	2.60	2.45E+02	4.36E+01	1.0000E+00	0.00	0.000E+00	0.000	0.000	0.000E+00	0.000	0.0000	2.505E+26	0.000E+00

SUMS: 4.0552 6.972E+15 4.2512 7.285E+15
 Energy buildup ratio = 1.048332 . Photon buildup ratio = 1.044897

Figure 2. Output from XPRT5 with additional parameters for comparison with ATRS.
 X-ray yield is one kiloton with a black-body temperature of 3.45 keV (4x10⁷K),
 altitude 150 kilofeet, range one kilometer, horizontal.

Additional XPRT type programs were generated to develop solutions for converse problems, such as ranges for a given calorie level to be deposited (program XQ5RDEP). These solutions are obtained by iteration and convergence. Solutions were limited to fireballs represented by a single black-body temperature. Combinations of multiple temperatures could be accommodated with a modest effort.

4.3. Comparison of results using ATR5 and XPRT5. Results of computations obtained by XPRT5 and ATR5 for two black-body temperatures (4×10^7 and 4×10^8 degrees Kelvin), four altitudes (80, 100, 150, and 200 kilofeet) and three horizontal ranges from source to target (1, 2, and 4 kilometers) are presented here. These parameters were selected because they were used in the benchmark calibration of XPRT5 by the MCNP program.⁵ The x-ray source is assumed to radiate one kiloton of energy in x rays. The results are tabulated in Table 6. ATR5 presents results for both fluence and current, with forward and backward results for each. These quantities are relevant for gamma-rays and neutrons which have considerable depth penetration into solid objects. For x rays, fluence and the backward component of current do not apply for the x-ray effects on the shell of a solid body of more than several mean free paths thickness. Consequently, only the forward components of the currents of the ATR5 results are compared here.

Examination of Table 6 shows excellent agreement between ATR5 and XPRT5 for all ranges at altitudes of 150 and 200 kft. At altitudes of 80 and 100 kft, ATR5 gives results up to 40% higher than XPRT5 for a black-body (BB) temperature of 3.45 keV, and gives results of up to 43% lower than XPRT5 for a BB temperature of 34.5 keV. The reasons for these differences can be explained in terms of three factors, air density, cross-sections, and representation of BB spectrum, which are discussed sequentially in the next three subsections.

4.3.1. Air density: ATR5 computes atmospheric density from a single formula which is very accurate up to 10 km altitude, but provides varying accuracy at higher altitudes. XPRT5 contains a built-in table of density values from the US Standard Atmosphere, 1976, for 90 different altitudes up to 300 km, from which densities at altitudes between data points are extrapolated by an exponential formula. XPRT5, therefore, calculates atmospheric density more precisely than ATR5, especially for the high endoatmosphere. The lower atmospheric density, and therefore the lower integrated path density, used by ATR5 at 80 and 100 kft altitude explains partially the higher transported x-ray current at 3.45 keV BB temperature. However, this factor does not explain why ATR5 shows a lower current for these altitudes at 34.5 keV BB temperature. These differences may be explained in terms of cross-sections and representation of BB spectrum.

Table 6. Comparison between ATR5 and XPRT5 of x-ray transport in the high endoatmosphere.

CASE NO.	CODE(1)	INTEGRATED MASS ALONG PATH (gm/cm ²)		PHOTON BUILDUP RATIOS (FORWARD CURRENT)				ENERGY BUILDUP RATIOS (FORWARD CUR.)		TOTAL PHOTON FORWARD CURRENT			TOTAL ENERGY FORWARD CURRENT (cal/cm ²)			
		XPRT5	ATR5	MCNP	XPRT4	XPRT5	ATR5	XPRT5	ATR5	XPRT5	ATR5	%(2)	MCNP	XPRT5	ATR5	%
1	470801	4.418	4.414	1.72	1.84	1.99	1.65	1.90	1.68	3.10E+1	3.98E+1	28.39	2.98E-01	2.99E-01	3.91E-01	30.86
2	470802	8.835	8.828	2.36	2.70	3.32	2.36	3.12	2.39	1.74E+1	2.27E+1	30.46	1.82E-02	1.92E-02	2.56E-02	33.33
3	470804	17.671	17.656	2.48	4.81	7.64	4.37	7.25	4.42	4.83E+1	6.03E+1	24.84	3.27E-04	6.00E-04	7.91E-04	31.83
4	471001	1.710	1.674	1.34	1.38	1.42	1.26	1.40	1.27	1.29E+1	1.53E+1	18.70	1.07E+0	1.07E+0	1.25E+0	16.93
5	471002	3.421	3.348	1.60	1.67	1.77	1.50	1.71	1.51	1.21E+1	1.56E+1	28.61	1.14E-01	1.12E-01	1.45E-01	29.12
6	471004	6.841	6.696	1.92	2.61	2.65	2.00	2.50	2.05	7.99E+1	1.10E+1	37.67	7.58E-03	8.40E-03	1.18E-02	40.48
7	471501	0.178	0.170	1.04	1.04	1.21	1.01	1.05	1.01	7.29E+1	7.36E+1	1.03	4.30E+0	4.25E+0	4.33E+0	1.86
8	471502	0.356	0.340	1.08	1.09	1.24	1.02	1.10	1.03	1.25E+1	1.30E+1	4.00	8.15E-01	8.07E-01	8.33E-01	3.27
9	471504	0.713	0.681	1.13	1.17	1.26	1.08	1.19	1.09	1.91E+1	2.09E+1	9.25	1.34E-01	1.38E-01	1.48E-01	7.48
10	472001	0.027	0.026	1.01	1.00	1.14	1.00	1.01	1.00	1.38E+1	1.38E+1	-0.29	6.52E+0	6.46E+0	6.52E+0	0.96
11	472002	0.055	0.051	1.01	1.01	1.16	1.00	1.01	1.00	2.88E+1	2.88E+1	0.17	1.46E+0	1.44E+0	1.46E+0	1.11
12	472004	0.110	0.102	1.02	1.02	1.19	1.00	1.03	1.01	5.63E+1	5.69E+1	1.01	3.10E-01	3.08E-01	3.14E-01	1.98
13	480801	4.418	4.414	2.92	2.58	2.85	2.27	1.95	1.91	2.45E+1	2.19E+1	-10.58	8.98E+0	7.88E+0	7.55E+0	-4.16
14	480802	8.835	8.828	5.57	5.13	6.16	4.03	3.56	3.05	6.37E+1	4.79E+1	-24.80	2.14E+0	1.88E+0	1.59E+0	-15.56
15	480804	17.671	17.656	13.88	15.72	19.59	9.60	9.62	6.14	1.30E+1	7.46E+1	-42.62	3.57E-01	3.69E-01	2.32E-01	-37.06
16	481001	1.710	1.674	1.61	1.55	1.57	1.44	1.30	1.33	2.20E+1	2.23E+1	1.27	7.96E+0	7.88E+0	7.91E+0	0.39
17	481002	3.421	3.348	2.30	2.19	2.30	1.93	1.68	1.66	5.89E+1	5.57E+1	-5.43	2.08E+0	1.97E+0	1.93E+0	-2.01
18	481004	6.841	6.696	3.70	3.85	4.52	3.12	2.79	2.46	1.62E+1	1.30E+1	-19.55	4.97E-01	4.92E-01	4.36E-01	-11.45
19	481501	0.178	0.170	1.06	1.06	1.13	1.04	1.02	1.03	2.13E+1	2.16E+1	1.65	7.87E+0	7.88E+0	7.75E+0	-1.65
20	481502	0.356	0.340	1.11	1.10	1.18	1.08	1.05	1.07	5.33E+1	5.41E+1	1.52	1.95E+0	1.97E+0	1.95E+0	-1.02
21	481504	0.713	0.681	1.18	1.21	1.27	1.18	1.11	1.15	1.34E+1	1.37E+1	2.01	4.77E-01	4.93E-01	4.96E-01	0.71
22	482001	0.027	0.026	1.01	1.03	1.11	1.00	1.00	1.01	2.12E+1	2.18E+1	2.73	7.84E+0	7.89E+0	7.72E+0	-2.15
23	482002	0.055	0.051	1.01	1.04	1.10	1.01	1.00	1.01	5.30E+1	5.43E+1	2.39	1.95E+0	1.97E+0	1.93E+0	-2.03
24	482004	0.110	0.102	1.02	1.05	1.11	1.02	1.01	1.02	1.33E+1	1.35E+1	1.81	4.86E-01	4.93E-01	4.84E-01	-1.83

(1) Code for BB temperature, altitude in kilofeet, and range in kilometers.

For example, 470801 indicates a BB temperature of 4.0E+7 degrees Kelvin, 80 kft altitude, and 1 km range (horizontal).

(2) Percent is calculated from (ATR5-XPRT5)/XPRT5.

4.3.2. Cross sections: Data are not available for ATR5 at this writing to compare all cross-sections used by ATR5 and XPRT5. Low-energy x-ray total cross sections are given in Table 7 of the RSIC presentation of ATR5.⁴ However, these are given for energy bands, e.g., 1 - 2 keV, and it is not specified whether the cross-section is chosen for the photon at the midpoint of the energy band or by some other criterion. If the energy midpoint is used for selection of the cross section, then the ATR5 cross sections are lower than those of XPRT5 by 3.4 to 8.3% for the energy groups between 1 and 10 keV, as shown by Table 7. If the ATR5 cross sections are consistently lower than the cross sections used by XPRT5 at higher photon energies than those compared in Table 7, these differences will also contribute to the higher x-ray currents computed by ATR5 from the 3.45 keV BB source at altitudes of 80 and 100 kft.

Attenuation coefficients for photons in air for the XPORT programs were computed using the PHOTX library of the National Institute of Standards and Technology, which will be used as the basis of File 23 for ENDF/B-VI.⁶ The computed coefficients are listed in Table 8. Coefficients for photons with energies less than one keV are not listed. It is curious that the ATR5 document⁴ lists photon cross sections for nine energy groups below one keV, the lowest group bounded by 0.1 - 0.2 keV. The mean free path of a one-keV photon in air is about 2 1/4 mm at sea level, and about 16 cm at 100 kft altitude, and the mean free paths of photons of lower energy are much shorter. For a black-body radiating with a temperature of only one keV, about 98% of the photons have energy greater than one keV.

4.3.3. Representation of BB spectra: Unlike the gamma-ray and neutron spectra from a nuclear detonation, the BB x-ray spectrum is fairly sharply peaked around the frequency for maximum power. In recognition of this fact, the XPORT programs calculate energy bin boundaries which spread out above and below the frequency of peak power corresponding to a selected BB temperature. The width of the bins are determined by integrating over the spectrum to sum up to a preselected percentage of the total energy radiated. As may be seen by examination of the two columns on the left side of Fig. 2, there are 5 bins each representing 10% of the source energy, 6 bins each representing 5%, etc., with a finer breakdown of bin structure toward the higher energy side of the spectrum. The central energy bin extends to 5% of the total energy to either side of the photon energy at peak emission power, which is at 9.73 keV in Fig. 2.

ATR5 uses a fixed-bin structure to represent the BB spectrum, as may be seen in the output shown in Fig. 3. The suitability of this representation will vary for different selections of BB temperature. The input parameters for the ATR5 solution shown

Table. 7. Comparison between ATR5 and XPRT5 of x-ray cross sections in air.

Energy Boundaries (keV)	Midpoint Energy (keV)	ATR5(a) Cross section cm ⁻¹	XPRT5 Cross section cm ⁻¹	Comparison % (b)
1.0 - 2.0	1.5	1.54E+00	1.46E+00	-5.48
2.0 - 3.0	2.5	3.25E-01	3.38E-01	3.85
3.0 - 4.0	3.5	1.25E-01	1.34E-01	6.72
4.0 - 5.0	4.5	6.23E-02	6.74E-02	7.57
5.0 - 6.0	5.5	3.41E-02	3.72E-02	8.33
6.0 - 7.0	6.5	2.19E-02	2.26E-02	3.10
7.0 - 8.0	7.5	1.42E-02	1.47E-02	3.40
8.0 - 9.0	8.5	9.54E-03	1.02E-02	6.47
9.0 - 10.0	9.5	6.85E-03	7.30E-03	6.16

(a) Assuming midpoint energy of energy group is used for cross section.

(b) Percentage computed from $(XPRT5 - ATR5)/XPRT5$

Table 8 Photon attenuation coefficients computed for air using the PHOTX library of the National Institute of Standards and Technology, which is to be incorporated in File 23 of ENDF/B-VI.

AIR

Constituents (Atomic Number:Fraction by Weight)
 6:0.00013 7:0.75522 8:0.23177 18:0.01288

Partial Interaction Coefficients and Total Attenuation Coefficients

PHOTON ENERGY (MeV)	SCATTERING		PHOTO-ELECTRIC ABSORPTION (cm ² /g)	PAIR PRODUCTION		TOTAL ATTENUATION	
	COHERENT (cm ² /g)	INCOHER. (cm ² /g)		IN NUCLEAR FIELD (cm ² /g)	IN ELECTRON FIELD (cm ² /g)	WITH COHERENT SCATT. (cm ² /g)	WITHOUT COHERENT SCATT. (cm ² /g)
1.000E-03	1.36E+00	1.04E-02	3.60E+03	0.00E-01	0.00E-01	3.61E+03	3.60E+03
1.500E-03	1.25E+00	2.12E-02	1.19E+03	0.00E-01	0.00E-01	1.19E+03	1.19E+03
2.000E-03	1.12E+00	3.34E-02	5.27E+02	0.00E-01	0.00E-01	5.28E+02	5.27E+02
3.000E-03	8.63E-01	5.75E-02	1.62E+02	0.00E-01	0.00E-01	1.62E+02	1.62E+02
3.203E-03	8.18E-01	6.20E-02	1.33E+02	0.00E-01	0.00E-01	1.34E+02	1.33E+02
18 K 3.203E-03	8.18E-01	6.20E-02	1.48E+02	0.00E-01	0.00E-01	1.49E+02	1.48E+02
4.000E-03	6.65E-01	7.77E-02	7.72E+01	0.00E-01	0.00E-01	7.79E+01	7.72E+01
5.000E-03	5.22E-01	9.33E-02	3.97E+01	0.00E-01	0.00E-01	4.03E+01	3.98E+01
6.000E-03	4.21E-01	1.05E-01	2.29E+01	0.00E-01	0.00E-01	2.34E+01	2.30E+01
8.000E-03	2.95E-01	1.21E-01	9.51E+00	0.00E-01	0.00E-01	9.92E+00	9.63E+00
1.000E-02	2.22E-01	1.32E-01	4.77E+00	0.00E-01	0.00E-01	5.12E+00	4.90E+00
1.500E-02	1.31E-01	1.47E-01	1.34E+00	0.00E-01	0.00E-01	1.61E+00	1.48E+00
2.000E-02	8.75E-02	1.56E-01	5.35E-01	0.00E-01	0.00E-01	7.78E-01	6.91E-01
3.000E-02	4.62E-02	1.62E-01	1.45E-01	0.00E-01	0.00E-01	3.54E-01	3.08E-01
4.000E-02	2.83E-02	1.63E-01	5.71E-02	0.00E-01	0.00E-01	2.49E-01	2.20E-01
5.000E-02	1.91E-02	1.61E-01	2.76E-02	0.00E-01	0.00E-01	2.08E-01	1.89E-01
6.000E-02	1.37E-02	1.59E-01	1.52E-02	0.00E-01	0.00E-01	1.87E-01	1.74E-01
8.000E-02	8.03E-03	1.52E-01	5.92E-03	0.00E-01	0.00E-01	1.66E-01	1.58E-01
1.000E-01	5.26E-03	1.46E-01	2.85E-03	0.00E-01	0.00E-01	1.54E-01	1.49E-01
1.500E-01	2.40E-03	1.32E-01	7.61E-04	0.00E-01	0.00E-01	1.36E-01	1.33E-01
2.000E-01	1.36E-03	1.22E-01	3.03E-04	0.00E-01	0.00E-01	1.23E-01	1.22E-01
3.000E-01	6.10E-04	1.06E-01	8.61E-05	0.00E-01	0.00E-01	1.07E-01	1.06E-01
4.000E-01	3.44E-04	9.51E-02	3.70E-05	0.00E-01	0.00E-01	9.55E-02	9.51E-02
5.000E-01	2.20E-04	8.69E-02	2.00E-05	0.00E-01	0.00E-01	8.71E-02	8.69E-02
6.000E-01	1.53E-04	8.04E-02	1.25E-05	0.00E-01	0.00E-01	8.06E-02	8.04E-02
8.000E-01	8.62E-05	7.06E-02	6.30E-06	0.00E-01	0.00E-01	7.07E-02	7.06E-02
1.000E+00	5.52E-05	6.35E-02	3.92E-06	0.00E-01	0.00E-01	6.36E-02	6.35E-02
1.022E+00	5.28E-05	6.29E-02	3.66E-06	0.00E-01	0.00E-01	6.29E-02	6.29E-02
1.250E+00	3.53E-05	5.68E-02	2.48E-06	1.78E-05	0.00E-01	5.69E-02	5.68E-02
1.500E+00	2.45E-05	5.16E-02	1.80E-06	9.85E-05	0.00E-01	5.17E-02	5.17E-02
2.000E+00	1.38E-05	4.41E-02	1.13E-06	3.92E-04	0.00E-01	4.45E-02	4.45E-02
2.044E+00	1.32E-05	4.35E-02	1.09E-06	4.22E-04	0.00E-01	4.39E-02	4.39E-02
3.000E+00	6.13E-06	3.47E-02	6.28E-07	1.12E-03	1.21E-05	3.58E-02	3.58E-02
4.000E+00	3.45E-06	2.89E-02	4.30E-07	1.82E-03	4.95E-05	3.08E-02	3.08E-02
5.000E+00	2.21E-06	2.50E-02	3.26E-07	2.44E-03	9.87E-05	2.75E-02	2.75E-02
6.000E+00	1.53E-06	2.21E-02	2.61E-07	3.00E-03	1.52E-04	2.52E-02	2.52E-02
7.000E+00	1.13E-06	1.98E-02	2.18E-07	3.49E-03	2.04E-04	2.35E-02	2.35E-02
8.000E+00	8.63E-07	1.81E-02	1.87E-07	3.94E-03	2.56E-04	2.23E-02	2.23E-02
9.000E+00	6.82E-07	1.66E-02	1.64E-07	4.35E-03	3.05E-04	2.13E-02	2.13E-02
1.000E+01	5.52E-07	1.54E-02	1.45E-07	4.72E-03	3.52E-04	2.04E-02	2.04E-02
1.100E+01	4.56E-07	1.43E-02	1.31E-07	5.05E-03	3.96E-04	1.98E-02	1.98E-02
1.200E+01	3.83E-07	1.35E-02	1.19E-07	5.36E-03	4.38E-04	1.92E-02	1.92E-02
1.300E+01	3.27E-07	1.27E-02	1.09E-07	5.65E-03	4.78E-04	1.88E-02	1.88E-02

ATR PROBLEM NUMBER 1 PROB 715 - X-RAY SUMMARY

X-RAY SOURCE INTERNAL BLACK BODY
 TOTAL ENERGY OUTPUT= 2.613E+28 KEV
 TOTAL OUTPUT=2.806E+27 X-RAY

SOURCE SPECTRUM

ENERGY(KEV)	X	X/KEV	ENERGY(KEV)	X	X/KEV
1.00E-01-1.00E+00	4.41E+25	4.90E+25	6.50E+01-7.50E+01	2.77E+21	2.77E+20
1.00E+00-1.00E+01	1.70E+27	1.89E+26	7.50E+01-9.00E+01	2.11E+20	1.41E+19
1.00E+01-1.50E+01	6.14E+26	1.23E+26	9.00E+01-1.05E+02	3.86E+18	2.58E+17
1.50E+01-2.00E+01	2.81E+26	5.62E+25	1.05E+02-1.20E+02	6.71E+16	4.47E+15
2.00E+01-2.50E+01	1.10E+26	2.19E+25	1.20E+02-1.40E+02	1.13E+15	5.67E+13
2.50E+01-3.00E+01	3.87E+25	7.74E+24	1.40E+02-1.60E+02	4.62E+12	2.31E+11
3.00E+01-3.50E+01	1.27E+25	2.55E+24	1.60E+02-1.90E+02	1.82E+10	6.07E+08
3.50E+01-4.50E+01	5.20E+24	5.20E+23	1.90E+02-2.20E+02	4.17E+06	1.39E+05
4.50E+01-5.50E+01	4.56E+23	4.56E+22	2.20E+02-2.60E+02	0.00E+00	0.00E+00
5.50E+01-6.50E+01	3.66E+22	3.66E+21	2.60E+02-3.00E+02	0.00E+00	0.00E+00

ATR PROBLEM NUMBER 1 PROB 715 - X-RAY SUMMARY

GROUND LEVEL .000KM, .000GM/CM**2, .000KFT, .000MILES
 HORIZ. RANGE RH= 1.000KM, .170GM/CM**2, 3.281KFT, .621MILES
 *SLANT RANGE RS= 1.000KM, .170GM/CM**2, 3.281KFT, .621MILES
 TARGET ALT. HT= 45.720KM,1033.844GM/CM**2,150.000KFT, 28.409MILES
 SOURCE ALT. HS= 45.720KM,1033.844GM/CM**2,150.000KFT, 28.409MILES
 *SLANT ANGLE AN= .000DEGREES (COS= 1.00000)
 *CALCULATED FROM OTHER COORDINATES

X-RAY SUMMARY

	UNCOLL.	TOTAL	BUILDUP	BACKWARD	FORWARD
TISSUE DOSE (RADS)	2.65E+06	2.68E+06	1.01E+00	1.05E+04	2.67E+06
SILICON DOSE (RADS)	2.36E+07	2.38E+07	1.01E+00	6.22E+04	2.37E+07
NUMBER FLUENCE(X/CM**2)	7.38E+15	7.50E+15	1.02E+00	3.01E+13	7.47E+15
NUMBER CURRENT(X/CM**2)	7.30E+15	7.35E+15	1.01E+00	1.42E+13	7.36E+15
ENERGY FLUENCE(X-CAL/CM**2)	4.33E+00	4.42E+00	1.02E+00	2.11E-02	4.40E+00
ENERGY CURRENT(X-CAL/CM**2)	4.28E+00	4.32E+00	1.01E+00	9.85E-03	4.33E+00
EXT. FLX. WT. ()	0.00E+00	0.00E+00	0.00E+00	0.00E+00	0.00E+00
AVERAGE ENERGY(CAL)	5.87E-16	5.89E-16	1.00E+00	7.02E-16	5.89E-16

Figure 3. Output from ATR5 for comparison with results from XPRT5 shown in Fig. 2. X-ray yield is one kiloton with a black-body temperature of 3.45 keV (4×10^7 K), altitude 150 kilofeet, range one kilometer, horizontal.

in Fig. 3 are the same as those for the XPRT5 solution shown in Fig. 2, both for a BB temperature of 3.45 keV (4×10^7 K). Considering that the two bins of lowest energy in ATR5 are subdivided into 18 finer divisions which are not shown in the ATR5 output, the spectrum is fairly well covered for this BB temperature.

In Figs. 4 and 5, solutions are given by ATR5 and XPRT5, respectively, for identical input parameters for a BB temperature of 34.5 keV (4×10^8 K). This temperature was chosen as an upper bound for the benchmark calculations of MCNP to provide calibration for the XPORT series of programs. For this BB temperature, ATR5 provides a much less detailed representation of the spectrum than XPRT5, and the energy bins do not go high enough to cover the top five bins shown by XPRT5 in Fig. 5. This difference in BB spectrum representation may account for some or most of the discrepancies between the results of ATR5 and XPRT5 at 34.5 keV shown in Table 6.

4.4. Conclusions and recommendations. From the above discussion, it is apparent that for high endoatmospheric calculations of x-ray transport, the XPORT programs calculate atmospheric density more accurately than ATR5, use coefficients that are more up-to-date than ATR5, and represent the black-body spectra with greater detail than ATR5. A comparison of running times has not been made, because both programs appear to run in negligible time (fractions of a second) on a modern desktop computer. For the reasons given above, it is recommended that the XPORT programs should be used in future calculations of x-ray transport in air for analyses involving the effect on components from x rays from nuclear detonations in the high endoatmosphere. It remains to be seen whether ATR6 will remedy the shortcomings of ATR5 for this application.

```

ATR PROBLEM NUMBER      1          PROB 810 - X-RAY SUMMARY
*****

X-RAY SOURCE INTERNAL BLACK BODY
TOTAL ENERGY OUTPUT= 2.613E+28 KEV
TOTAL OUTPUT=2.788E+26 X-RAY

SOURCE SPECTRUM
ENERGY(KEV )      X      X/KEV  ENERGY(KEV )      X      X/KEV
1.00E+01-1.00E+00 4.82E+22 5.35E+22 6.50E+01-7.50E+01 2.11E+25 2.11E+24
1.00E+00-1.00E+01 4.41E+24 4.90E+23 7.50E+01-9.00E+01 2.92E+25 1.95E+24
1.00E+01-1.50E+01 5.08E+24 1.02E+24 9.00E+01-1.05E+02 2.55E+25 1.70E+24
1.50E+01-2.00E+01 6.59E+24 1.32E+24 1.05E+02-1.20E+02 2.15E+25 1.43E+24
2.00E+01-2.50E+01 7.82E+24 1.56E+24 1.20E+02-1.40E+02 2.27E+25 1.14E+24
2.50E+01-3.00E+01 8.82E+24 1.76E+24 1.40E+02-1.60E+02 1.68E+25 8.40E+23
3.00E+01-3.50E+01 9.60E+24 1.92E+24 1.60E+02-1.90E+02 1.66E+25 5.53E+23
3.50E+01-4.50E+01 2.08E+25 2.08E+24 1.90E+02-2.20E+02 9.53E+24 3.18E+23
4.50E+01-5.50E+01 2.18E+25 2.18E+24 2.20E+02-2.60E+02 6.39E+24 1.60E+23
5.50E+01-6.50E+01 2.18E+25 2.18E+24 2.60E+02-3.00E+02 2.73E+24 6.83E+22
*****

ATR PROBLEM NUMBER      1          PROB 810 - X-RAY SUMMARY
*****

GROUND LEVEL      .000KM,   .000GM/CM**2,   .000KFT,   .000MILES
HORIZ. RANGE RH= 1.000KM, 1.674GM/CM**2, 3.281KFT, .621MILES
*SLANT RANGE RS= 1.000KM, 1.674GM/CM**2, 3.281KFT, .621MILES
TARGET ALT. HT= 30.480KM,1024.088GM/CM**2,100.000KFT, 18.939MILES
SOURCE ALT. HS= 30.480KM,1024.088GM/CM**2,100.000KFT, 18.939MILES
*SLANT ANGLE AN= .000DEGREES (COS= 1.00000)
*CALCULATED FROM OTHER COORDINATES
*****

X-RAY SUMMARY
UNCOLL. TOTAL BUILDUP BACKWARD FORWARD
TISSUE DOSE (RADS ) 9.22E+04 1.53E+05 1.66E+00 1.35E+04 1.40E+05
SILICON DOSE (RADS ) 2.55E+05 4.94E+05 1.93E+00 6.06E+04 4.33E+05
NUMBER FLUENCE( X/CM**2 ) 1.56E+15 2.74E+15 1.75E+00 2.49E+14 2.49E+15
NUMBER CURRENT( X/CM**2 ) 1.55E+15 2.11E+15 1.37E+00-1.12E+14 2.23E+15
ENERGY FLUENCE( X-CAL/CM**2 ) 6.01E+00 9.15E+00 1.52E+00 5.62E-01 8.59E+00
ENERGY CURRENT( X-CAL/CM**2 ) 5.94E+00 7.66E+00 1.29E+00-2.48E-01 7.91E+00
EXT. FLX. WT. ( ) 0.00E+00 0.00E+00 0.00E+00 0.00E+00 0.00E+00
AVERAGE ENERGY(CAL ) 3.84E-15 3.34E-15 8.70E-01 2.26E-15 3.45E-15
*****

```

Figure 4. Output from ATR5 for comparison with results from XPRTs shown in Fig. 5. X-ray yield is one kiloton with a black-body temperature of 34.5 keV (4×10^8 K), altitude 100 kilofeet, range one kilometer, horizontal.

APPROXIMATION FOR X-RAY TRANSPORT IN AIR
 BASIC Program XPRTSATR, by Carsten. M. Naaland, ORNL, 1989

INPUT: Yield of nuclear warhead: 1 kilotons; Fraction of yield emitted as x rays: 1
 Blackbody x-ray temperature: 34.4693 keV (4E+08 deg. Kelvin)
 Altitude of target: 100 kilofeet (30.48 kilometers)
 Slant range to detonation: 1 kilometers
 Slant angle (to horizontal) from target to detonation: 0 degrees

OUTPUT: Height of detonation above or below (negative) target: 0 kilofeet
 Air density at target altitude: 1.710322E-05 gm/cm³
 Integrated air mass along slant path: 1.710322 gm/cm²
 Total unattenuated x ray deposition at target: 7.957747 cal/cm²
 Photon energy at peak emission power: 97.25301 keV
 Total x-ray energy output: 2.609E+28 keV; Total number of source x-ray photons, 2.755035E+26
 Number of transmitting windows: 25
 PARAM = 82.57462 ; G = .7150768

ENERGY DEPOSITION PER WINDOW:

Percent of source energy	Photon energy (keV)	Nu (cm ² /gm)	Number of RFPs	Buildup factor	Uncollided flux (Energy) (cal/cm ²)	Uncollided flux (Photons) (#/cm ²)	Fraction of total unc. flux	Flux w/buildup (Energy) (cal/cm ²)	Flux w/buildup (Photons) (#/cm ²)	Fraction of total	Photon buildup	No. of source photons	Photons per vacuum photon
0.2250	462.55	8.99E-02	1.54E-01	1.1605E+00	0.02	8.660E+11	0.003	0.015	8.660E+11	0.002	1.0000	1.269E+23	8.575E-01
0.3125	387.04	9.68E-02	1.65E-01	1.1853E+00	0.02	1.421E+12	0.003	0.021	1.421E+12	0.003	1.0000	2.107E+23	8.476E-01
0.3125	359.58	9.96E-02	1.70E-01	1.1972E+00	0.02	1.522E+12	0.003	0.021	1.522E+12	0.003	1.0000	2.267E+23	8.434E-01
0.6250	334.87	1.02E-01	1.75E-01	1.2088E+00	0.04	3.252E+12	0.007	0.042	3.252E+12	0.005	1.0000	4.869E+23	8.393E-01
0.6250	314.71	1.05E-01	1.80E-01	1.2192E+00	0.04	3.446E+12	0.007	0.042	3.446E+12	0.005	1.0000	5.181E+23	8.357E-01
1.2500	294.01	1.08E-01	1.84E-01	1.2313E+00	0.08	7.342E+12	0.014	0.084	7.473E+12	0.011	1.0178	1.109E+24	8.466E-01
1.2500	274.98	1.10E-01	1.89E-01	1.2446E+00	0.08	7.816E+12	0.014	0.084	7.977E+12	0.011	1.0205	1.186E+24	8.452E-01
2.5000	254.94	1.13E-01	1.94E-01	1.2598E+00	0.16	1.678E+13	0.027	0.171	1.755E+13	0.022	1.0459	2.558E+24	8.619E-01
2.5000	235.86	1.16E-01	1.99E-01	1.2756E+00	0.16	1.804E+13	0.027	0.172	1.897E+13	0.022	1.0518	2.765E+24	8.622E-01
5.0000	215.16	1.20E-01	2.05E-01	1.2946E+00	0.32	3.930E+13	0.053	0.353	4.275E+13	0.045	1.0878	6.063E+24	8.861E-01
5.0000	194.89	1.24E-01	2.12E-01	1.3206E+00	0.32	4.308E+13	0.053	0.354	4.744E+13	0.045	1.1011	6.693E+24	8.906E-01
5.0000	179.07	1.28E-01	2.19E-01	1.3555E+00	0.32	4.659E+13	0.053	0.359	5.227E+13	0.046	1.1219	7.285E+24	9.017E-01
5.0000	165.85	1.31E-01	2.25E-01	1.3877E+00	0.32	5.000E+13	0.052	0.364	5.733E+13	0.046	1.1465	7.865E+24	9.159E-01
10.0000	149.06	1.36E-01	2.33E-01	1.4329E+00	0.63	1.103E+14	0.104	0.770	1.347E+14	0.098	1.2212	1.750E+25	9.674E-01
10.0000	130.04	1.42E-01	2.43E-01	1.4779E+00	0.62	1.252E+14	0.103	0.789	1.584E+14	0.100	1.2646	2.006E+25	9.919E-01
10.0000	113.16	1.48E-01	2.54E-01	1.5251E+00	0.62	1.424E+14	0.102	0.813	1.875E+14	0.103	1.3169	2.306E+25	1.022E+00
10.0000	97.25	1.55E-01	2.66E-01	1.5832E+00	0.61	1.637E+14	0.100	0.839	2.251E+14	0.106	1.3757	2.683E+25	1.055E+00
10.0000	81.32	1.65E-01	2.82E-01	1.6809E+00	0.60	1.925E+14	0.099	0.868	2.786E+14	0.110	1.4471	3.208E+25	1.091E+00
5.0000	68.55	1.77E-01	3.03E-01	1.7641E+00	0.29	1.119E+14	0.048	0.424	1.616E+14	0.054	1.4439	1.903E+25	1.067E+00
5.0000	59.07	1.89E-01	3.23E-01	1.8394E+00	0.29	1.273E+14	0.047	0.436	1.926E+14	0.055	1.5136	2.208E+25	1.096E+00
2.5000	50.94	2.06E-01	3.52E-01	1.9000E+00	0.14	7.167E+13	0.023	0.212	1.087E+14	0.027	1.5168	1.280E+25	1.067E+00
2.5000	44.63	2.28E-01	3.90E-01	1.9310E+00	0.13	7.875E+13	0.022	0.216	1.260E+14	0.027	1.6005	1.461E+25	1.084E+00
2.5000	36.98	2.74E-01	4.69E-01	1.9661E+00	0.12	8.783E+13	0.021	0.219	1.545E+14	0.028	1.7593	1.764E+25	1.101E+00
2.5000	26.04	4.66E-01	7.97E-01	1.7478E+00	0.09	8.984E+13	0.015	0.211	2.113E+14	0.027	2.3516	2.505E+25	1.060E+00
0.4000	13.62	2.12E+00	3.63E+00	1.0000E+00	0.00	0.000E+00	0.000	0.000	4.177E+11	0.000	0.0000	7.665E+24	6.848E-03
SUMS:					6.0700	1.541E+15		7.8794	2.202E+15				
Energy buildup ratio = 1.298079 . Photon buildup ratio = 1.428948													

Figure 5. Output from XPRT5 for comparison with results from ATR5 shown in Fig. 4. X-ray yield is one kiloton with a black-body temperature 34.5 keV (4×10^8 K), altitude 100 kilofeet, range one kilometer, horizontal.

REFERENCES

1. Beta spectrum obtained through private communication from Nichols Research Corporation, Huntsville, AL, 15 December 1989.
2. "Calculated beta-ray spectra from decay of fission products produced by thermal-neutron fission of ^{235}U ," J.K. Dickens, *Physics Letters*, Volume 113B, No. 3, 17 June, 1982, pp. 201-204.
3. *TREM TECHNICAL MANUAL, Volume II: TREM Models and Code Manual*, NRC-TR-89-211, Stan Berry, Nichols Research Corporation, Huntsville, AL, revised 19 February 1990.
4. *ATR5, Models of Radiation Transport in Air: Documentation for CCC-179/ATR5 Code Package*, F. Dolatshahi. et al., contributed by Science Applications International Corporation, San Diego, CA, April 1989, RSIC Computer Code Collection, Radiation Shielding Information Center, Oak Ridge National Laboratory, Oak Ridge, TN.
5. "An Approximation for Black-body x-Ray Transport in Air," C. M. Haaland, R. T. Santoro, and J. M. Barnes, *Applied Radiation and Isotopes*, Vol. 41, No. 4, pp. 407-415, 1990.
6. "Photon Cross Sections for ENDF/B-VI," D. K. Trubey, M. J. Berger, and J. H. Hubbell, in *Advances in Nuclear Engineering Computation and Radiation Shielding*," Volume 1, April, 1989, American Nuclear Society, Inc., LaGrange Park, IL 60525.

INTERNAL DISTRIBUTION

- | | |
|-----------------------|------------------------------|
| 1. B. R. Appleton | 19-23 R. C. Ward |
| 2. D. E. Bartine | 24. J. E. White |
| 3. J. K. Dickens | 25-29. EPMD Reports Office |
| 4-8. C. M Haaland | 30-31. Laboratory Records |
| 9-13. D. T. Ingersoll | Department |
| 14. J. R. Merriman | 32. Laboratory Records |
| 15. J. V. Pace III | ORNL-RC |
| 16. R. T. Santoro | 33. Document Reference |
| 17. M. S. Smith | 34. Central Research Library |
| 18. W. B. Snyder, Jr. | 35. ORNL Patent Section |

EXTERNAL DISTRIBUTION

36. Director, Defense Nuclear Agency, ATTN: STDB (Dr. David L. Auton), 6801 Telegraph Road, Alexandria Virginia 22310
37. Stanley R. Berry, Nichols Research Corporation, 404 Memorial Parkway, Huntsville, Alabama 35815-1502
38. N. Ricky Byrn, Nichols Research Corporation, 404 South Memorial Parkway, Huntsville, Alabama 35815-1502
39. P. Dolan, Lockheed Missile & Space Co., Post Office Box 3504, Sunnyvale California 94088-3504
40. F. Dolatshahi, SAIC, 10260 Campus Point Drive, San Diego, California 92121
41. J. J. Dorning, Department of Nuclear Engineering and Engineering Physics, Thornton Hall, University of Virginia, Charlottesville, Virginia 22901
42. W. Edwin Farley, Jr., Lawrence Livermore National Laboratory, Post Office Box 808, Livermore, California 94551
43. Commanding Officer, Defense Nuclear Agency, ATTN: RARP (Major R. A. Kehlet), 6801 Telegraph Road, Alexandria, Virginia 22310
44. D. C. Kaul, SAIC 10260 Campus Point Drive, San Diego, California 9212
45. James E. Leiss, Rt. 2, Box 142C, Broadway, Virginia 22815
46. Neville Moray, Department of Mechanical and Industrial Engineering, University of Illinois, 1296 West Green Street, Urbana, Illinois 61801
47. Lewis T. Smith, Teledyne Brown Engineering, MS 506, Cummings Research Park,
48. E. Straker, Science Application, Inc., Post Office Box 2351, La Jolla, California 92038

49. Robert Young, Defense Nuclear Agency, 6801 Telegraph Road, Alexandria, Virginia 22310
50. Mary Wheeler, Department of Mathematical Sciences, Post Office Box 1892, Houston , Texas 77251
51. Office of Assistant Manager for Energy Research and Development, Department of Energy, Oak Ridge Operations, P. O. Box 2001, Oak Ridge, Tennessee 37831
- 52-61. Office of Scientific and Technical Information, P. O. Box 62, Oak Ridge, Tennessee 37830